Technical note on incorporating natural variability in master recession curves

Thomas A McMahon[1], Rory J Nathan[1], Richard George[2]

[1] Department of Infrastructure Engineering, The University of Melbourne, Parkville, 3010, Victoria, Australia
[2] Department of Primary Industries and Regional Development, PO Box 1231, Bunbury, 6231, WA, Australia

Correspondence to: Rory Nathan (rory.nathan@unimelb.edu.au)

Abstract. In this technical note, we hypothesise that the master recession curve (MRC) is a continuum rather than a single average curve and the natural variability as evidenced in the range of MRCs represents aleatory uncertainty across the continuum and is the result of antecedent hydroclimatic and heterogeneous storage conditions in unconfined aquifer/s supplying streamflow. For four streams, representing the range of Australian hydrology, master recession curves were computed for five aleatory conditions (90, 75, 50, 25 and 10 percentiles) using the correlation technique. Observed recessions were superimposed on the plots confirming that the continuum of MRCs represented the observed conditions. For one catchment, the Northern Arthur River (437 km^2 in Western Australia yielding 2.7 mm runoff per year), field data were available. These were used to develop a two-store qualitative model that supports the continuum concept.

1 Introduction

This technical note describes for periods of no rainfall a comparison between daily master recession curves (MRCs) of a stream, computed using the correlation approach (Langbein, 1938; Federer, 1973; Boughton, 2015), and observed daily streamflow recessions for four catchments representative of the Australian hydrologic landscape.

MRCs, which are plots of discharge against time, are unique representations of streams, catchments and their associated contributing aquifer systems. The shape of an MRC depends on the connected aquifers contributing to the stream. The shape is also affected by evapotranspiration from the discharging aquifer through deep-rooted vegetation, by transmission losses in the stream which include evaporation from the stream water surface, evapotranspiration from the directly connected riparian zone, and from the stream as seepage to the bed, and at high flows recharge to the banks (McMahon and Nathan, 2021). In this paper, interflow, which is rainfall that on infiltrating moves laterally through the upper soil returning to the surface downslope prior to joining the stream, is considered part of the MRC. However, any rainfall that becomes surface runoff and remains so is not considered part of the baseflow recession process where baseflow is the combination of groundwater and delayed sub-surface flows (Shaw, 1994).

Master recession curve analyses have been part of the hydrologic tool kit for the past ninety years. The master recession curve was known initially as a composite recession curve (Linsley et al., 1958, p150) or a normal recession curve (Chow et al., 1988, p134). According to Chow et al. (1988, p132), Horton (1933) was the first person to describe the normal depletion curve (or master baseflow recession curve as noted by Chow et al., (1988, p134)). The literature on MRCs is extensive and covers reviews, procedures to estimate MRCs, and discussions of their uses. The major reviews include Toebes and Strang (1964), Hall (1968), Tallaksen (1995), Smakhtin (2001) and Brodie and Hostetler (2005).

Several methods are available to construct an MRC. Two well-known procedures are the correlation method of Langbein (1938) and the matching strip method of Snyder (1939). Other procedures include the tabulating method of Johnson and Dils (1956), the double exponential recession equation (Snyder, 1962), the least squares two recession constants model (James and Thompson, 1970), ordination of discharge related to daily recession slope on a monthly or half-monthly partition (Federer, 1973), weighted least squares applied to a multiple source concept (Pereira and Keller, 1982), and a combined iterative and graphical technique assuming a multiple source model (Petras, 1986). Arnold et al. (1995) considered daily data for months of low evapotranspiration and used a digital filter to separate baseflow, which was further analysed to produce an MRC. Boughton (1995) developed computer programmes to partition streamflow into baseflow segments and to combine segments into an MRC. Nathan and McMahon (1990) evaluated the correlation and the matching strip methods based on 186 catchments in southeastern Australia, noting that matching strip method was found to be the better approach. Brown (1965) prepared MRCs for Beaver Creek in Arizona and concluded that the recession slopes were much steeper in summer than in winter. Lamb and Beven (1997) developed an interactive software package, based on the matching strip method, and excluded not only recession periods of precipitation but also those in which the potential evaporation is high. In considering an MRC, Chapman (2003) assessed seven models, but only two can be considered equivalent to a master recession curve as described previously because the other five include a parameter that assumes significant recharge continues through the recession period. Based on an analysis of a hard rock aquifer, Dewandel et al. (2003) concluded that for shallow aquifers with a horizonal base a quadratic equation best fits long recessions whereas an exponential equation underestimates the dynamic volume of the aquifer. Sujono et al. (2004), who compared a master recession curve with a wavelet transformation on a semi-log plot, concluded that the wavelet procedure produced promising results. Also, Berhail et al. (2012) applied wavelet methodology to construct MRCs for two streams in Algeria. Mizumura (2005) carried out a theoretical analysis of MRCs using applied kinematic and diffusion wave models with and without lateral flow. Unfortunately, the plots are log-log (Q ~ t) making it difficult to compare the results with the usual log-linear plots. Working in fractured mountain areas, Millares et al. (2009) identified two MRCs, one was a quick response through the fractured material whereas the other was a slow response with

linear behaviour. Posavec et al. (2010) adopted a Visual Basic for Application program to process the matching strip method. Griffiths and McKerchar (2015, 2010) examined a deterministic model and a statistical model to predict MRC at ungauged sites. Based on application to 10 catchments, they concluded that further development is required. Fiorotto and Caroni (2013) developed a statistical framework for constructing an MRC explicitly providing for uncertainty, while Gregor and Malik

65   (2012) adopted a genetic algorithm approach. Boughton (2015) used the correlation approach following Federer (1973) basing his MRC on binned ratios of Q_j/Q_{j-1} from a sub-set of daily streamflow (Q_j is streamflow on day j) and estimated the average ratio in each bin. Discussing Boughton's (2015) method, French (2015) suggested using the maximum values rather than the average in each of Boughton's bins. In specifying daily MRCs, Ambroise (2016) adopted a second-order hyperbolic function. Nimmo and Perkins (2018) provide an expert-guided structure approach to estimate both streamflow and water table MRCs

70   (defined as $\frac{dR}{dt} = f(R)$ where R is a measured response) for average and episodic conditions and a range of time-steps. Carlotto and Chaffe (2019) packaged a set of automatic tools (MRCPTool) to analyse recession periods. Seasonal importance is evident in the MRC analysis of Yang et al. (2019). Duncan (2019) adopted, inter alia, the Toebes and Strang (1964) equation to estimate an MRC. Singh and Griffiths (2021) used the Lamb and Beven (1997) matching strip methods to develop an MRC based on a three-parameter generalised equation for estimation of an MRC in an ungauged catchment. Chen et al. (2012) and

75   Kavousi and Raeisi (2015) dealt with the special case of Karst aquifers. O'Brien et al. (2014) and Margreth et al. (2024) tested several procedures while Latuamury et al. (2024) compared the application of seven recession functions with observed flows which showed the models differed from the exponential reservoir model. In our analysis that follows, we implemented the correlation method which is most suitable to develop MRCs curves representing variability. The correlation procedure was initially proposed by Langbein (1938) and adopted or recommended by others (Knisel, 1963; Hall, 1968; Beran and Gustard,

80   1977; Institute of Hydrology, 1980; Smakhtin, 2001; Boughton, 2015; Yang et al. 2019: Trotter et al., 2024).

Nowhere in these developments and applications is the variability in the recession rate treated as a function of antecedent conditions, which lead us to characterise formally the natural variability inherent in the rates of streamflow depletion in the absence of rainfall as aleatory uncertainty, which we represent as MRC percentiles. We apply our approach to four catchments

85   representative of a wide range of hydroclimatology in Australia and compare the derived MRCs to observed recessions. Our approach is parsimonious in that it uses the time-based analysis ($Q \sim t$) of Horton (1933), Horner and Flynt (1936) and Barnes (1939) rather than the time-derivative-based analysis ($-dQ/dt \sim Q$) following Brutsaert and Nieber (1977). In this context we note the comment of Kim at al. (2023, Abstract) that "…data points in the recession plot, the plot of $-dQ/dt$ versus Q, typically form a wide point cloud due to noise and hysteresis in the storage-discharge relationship, and it is still unclear what information

90   we can extract from the plot and how to understand the information." Our analysis builds on McMahon and Nathan (2025) in the $Q \sim t$ space in which the MRC variability is considered in terms of aleatory uncertainty.

2 Adopted approach

Our analysis is in two steps. We first develop a continuum of MRCs based on their non-exceedance percentiles using the correlation method (Section 2.1), and then we superimpose observed recessions on the continuum of MRCs to illustrate the representativeness of the observed behaviour (Section 2.2). The application of these two steps is outlined in Section 3 and results are discussed in Section 4.

2.1 Development of Master Recession Curve

An MRC is commonly shown as a plot of daily streamflow (logarithmic scale) as a function of time as in Figure 1. From A to B, the MRC is upwardly concave until the flow reaches the maximum recession constant (B) (location of minimum recession slope) after which the logarithm of flow decreases linearly (B to C). If there is transmission loss (stream evaporation or evapotranspiration from the adjacent riparian zone or leakage to the stream bed) the MRC follows B to D. The difference in the curves (B - D) and (B - C) is transmission loss, as defined by Boughton (2015).

Although the term 'master recession curve' was not introduced into the hydrology literature until 1964 by Toebes and Strang (1964), the MRC was initially called a "normal depletion curve" by Horton (1933), "groundwater depletion curve" by Grundy (1951) and a "composite recession curve" by Linsley et al. (1958).
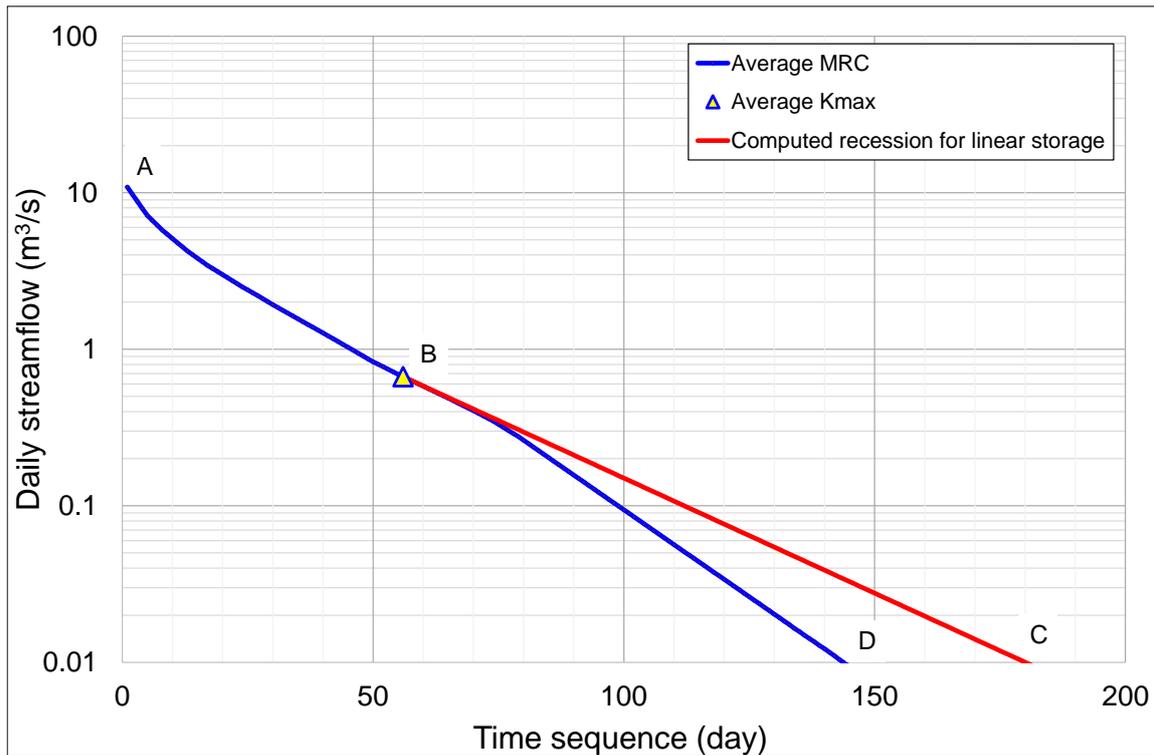
Figure 1 Example of an average Master Recession Curve (MRC) for Gibbo River at Gibbo Park (401207) including baseflow for a linear model and the average maximum recession coefficient (Kmax). ABC is an average MRC plot whereas ABD is an average MRC incorporating the effect of transmission loss.

An MRC represents the average rate of decline in streamflow following isolated periods of rainfall after surface runoff contributions have ceased. The average rate of decline is determined from the analysis of many individual recessions. The recession shape at any point in time depends on the initial water content of the unconfined aquifer and other sub-surface processes that together feed the stream. Also, as noted above, transmission losses affect recession shape. The initial water content of the aquifer/s and sub-storage systems is a result of the preceding climate and aquifer antecedent storage, as observed by Bart and Hope (2014). In our analysis we acknowledge that while the MRC is normally recognised as representing the average rate of decline, it is sensible to characterise the natural variability (or aleatory uncertainty) in the MRC that arises from variable antecedent hydroclimatic conditions and heterogeneous storage conditions in the aquifer. Hence, in contrast to others (Tallaksen, 1995; Duncan, 2019), our concept of an MRC of a stream is that it is a continuum of curves that results from the initial water content of the aquifers feeding the stream and from the spatial heterogeneity in their physical

5

configuration. These storages range from being full following a very wet period to a near empty condition following a long dry period. In our analysis, these two extreme conditions are represented by MRCs for 90%'ile (90th percentile) and 10%'ile non-exceedance frequency curves respectively. Three intermediate conditions are also included: 75%'ile represents a moderate wet period whereas 25%'ile is for a moderate dry period. The 'typical' initial condition is represented by a 50%'ile MRC. Here, we express variability in terms of a non-exceedance probability rather than in terms of a physical variable, for example, antecedent rainfall. That is, in some catchments it might be reasonable to expect that an individual recession might follow an MRC that is exceeded 30% of the time, and another might follow an MRC that is exceeded 70% of the time. Our approach is not inconsistent with Fiorotto and Caroni (2013), who analysed the structure of the recession curve within a stochastic rather than in a deterministic framework, and follows our recent paper, McMahon and Nathan (2025).

An important parameter associated with an MRC is the maximum recession constant (K_{max}). It has been used by many researchers under different guises. For example, it is related to the characteristic time (Brutsaert and Lopez, 1988), or to residence time (Chapman, 2003). Boughton (2015) utilised the maximum recession constant in estimating transmission losses in streams and McMahon and Nathan (2025) utilised K_{max} as a key to their procedure to estimate hydraulic properties of unconfined aquifers from daily streamflow data.

It is rare for observed daily streamflows to be available for long periods without the intrusion of rainfall or observational tolerance issues, or measurement malfunction, and so plots of actual recessions (streamflow volume Q vs time t) rarely show a complete shape of the recession. For example, Figure 2 of Yeh and Huang (2019) illustrates these points. For their 1992 data, there is no recession for days 14 and 15, nor for days 16 and 17 as the estimated flows are equal within each pair. Furthermore, presumably because of rainfall, the recessions do not extend beyond day 17 (1992 data) and day 13 (2012 data). Virtually all investigators are confronted with these problems.

The non-exceedance percentile values for the MRC are estimated from binned values of daily K_j (recession constant) and Q_j pairs following the correlation method (Hall, 1968; Beran and Gustard, 1977; Boughton, 2015) which is adopted herein to compute an MRC. The key steps in the correlation approach are:

1. Daily recession constants (K_j) (where $K_j = Q_j/Q_{j-1}$, for $0 < K_j < 1$,) and Q_j (daily discharge at time j) are ranked as pairs (by Q_j) after values potentially affected by rainfall are discarded. The number of rain-impacted days to be discarded is a function of catchment area guided by Linsley et al. (1982, Equation 7-4). We have not included adjustment for data imprecision (Rupp et al., 2009) because we compare the computed MRC with observed recession data.

2. The ranked pairs are binned using constant bin sizes varying between 50 and 200 items (Figure 2).

3. For each bin and based on K_j, a range of non-exceedance percentiles (10% percentile, 25%'ile, 50%'ile, 75%'ile and 90%'ile) are computed. Figure 2 is an example of the bins showing K_j and Q_j values. To provide for varying initial conditions according to catchment wetness (and hence the initial averaged state of the unconfined aquifer storage), the 10%'ile, 25%'ile, …, and 90%'ile daily Q values are also estimated. Thus, the initial 10%'ile discharge is associated with the 10%'ile MRC, and so on.

4. The final step is to construct the continuum of MRCs. For a given percentile (say 90%'ile), the MRC is estimated as described by Boughton (2015, p. 45). Begin at the highest value of daily flow in the record of K_j plausible values defined by point 1 above. The next highest value Q in the MRC is calculated by multiplying the highest value by the 90%'ile rate of recession in the daily flow range of the highest flow. The next value is calculated by multiplying that value by the 90%'ile rate of recession in the daily flow range of the result. This is continued until the flow rate becomes smaller than the lowest flow rate in the record. This process is carried out for each percentile. An example of an MRC computed in this manner is presented as Figure 3.

5. The maximum recession constant for a given percentile is obtained from the binned values (Figure 2); example values are plotted in Figure 3.
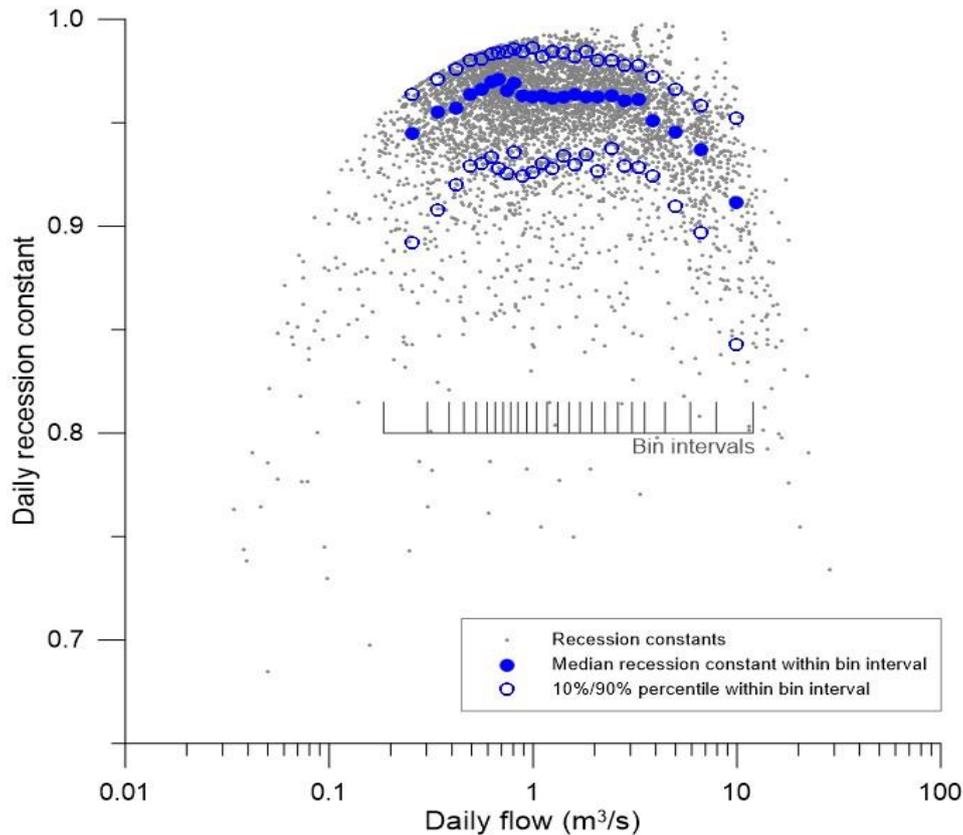
Figure 2 Relationship between daily recession constant and daily flow for Gibbo River at Gibbo Park 110 **(401217) showing median,**
10%ile, and 90%ile recession constants in each bin of 200 values.

2.2 Selection and superposition of recessions

In accepting the daily observed recessions for plotting (as in Figure 3), we adopted the following guidelines:

1. Choose at least ten consecutive decreasing daily discharges that are for days unimpacted by rainfall. The first x days are not used in plotting the observed recession to reduce the potential for surface runoff to affect the recession. Here, 'x' days is defined by Linsley et al. (1982, Equation 7-4).

2. Acceptable recessions superimposed on the MRC (log Q (ordinate) versus time (abscissa) graph) should be gently concave (representing non-linearity), convex (after the maximum recession constant, i.e. affected by transmission loss), or a straight line from the maximum recession constant, i.e. the discharge is from a linear storage system not exhibiting transmission

8

185   loss. This latter condition is most unlikely as all streams will have evaporation/evapotranspiration loss, although in some cases the loss may be too small to affect the daily discharge estimates.

3. Discharges that diverge upward from the main curve are deleted. These could occur at either end of the plotted observed daily time-series. The earlier values may be the result of some residual surface runoff not being removed by waiting x days before the plot begins. Or the last value (or last few values) could be the result of catchment rainfall (and, therefore, 190   runoff) not identified in the observed rainfall data.

4. The resulting plotted data should have at least seven consecutive recessive data points, i.e. the recession does not include days with equal discharge. This seven-day limit is subjective and there is a trade-off between sufficient data points to define a recession and sufficient recessions to define portions of the master recession curve. Others have used 12 days (Hameed et al., 2023), 10 days (van Dyke, 2010), 7 days (Whitaker et al., 2022), 6 days (Gao et al., 2023) and 5 days 195   (Parra et al., 2023).

2.3 Study catchments

The comparison between the computed MRCs and observed recessions was made for four streams as set out in Table 1. They cover the hydrology across Australia as defined by mean annual catchment runoff from about 3 to 2000 mm/year.

200

As noted above, the number of raindays to be eliminated prior to plotting the recessions is a function of catchment area and for Gibbo, Northern Arthur and South Johnstone Rivers three days were eliminated whereas for Myall River the initial four days of recessions were eliminated.

205

Table 1 Attributes of study catchments and details of plotted recessions

River name and gauging station	Station reference no.	Latitude, Longitude	Köppen class#	Area (km^2)	Data period	Mean annual runoff (mm/year)	Annual Cv*	No. of plausible recessions ≥ 7 days	No. of plotted recessions
Northern Arthur River @ Lake Toolibin Inflow	609010	32.905°S, 117.614°E	Csa	437	Sep '78 - Feb '22	2.7	2.6	24	22
Myall Creek @ Molroy	418017	29.799°S, 150.583°E	Cfa	865	Dec '78 - Feb '22	37	1.28	63	55
Gibbo River @ Gibbo Park	401217	36.756°S, 147.709°E	Cfb	390	Aug '71 - Feb '22	283	0.53	65	64
South Johnstone River @ Upstream Central Mill	112101B	17.609°S, 145.979°E	Af	398	Nov '74 - Feb '22	2027	0.38	32	30

Csa: temperate, dry hot summer; Cfa: temperate, no dry season, hot summer; Cfb temperate, no dry season, warm summer; Af: tropical, rainforest (Peel et al., 2007)

* Cv is coefficient of variation of annual streamflows

210

3 Application

For each stream, MRCs were computed (as set out in Section 2.1) for five non-exceedance frequencies: 10%, 25%, 50%, 75% and 90%'ile values, representing very dry initial conditions (10%'ile) to very wet initial conditions (90%'ile). The resulting MRCs obtained for Gibbo River at Gibbo Park are shown in Figure 3 in which the observed recessions are superimposed on

215   the computed MRCs for the five frequency values. This was done manually by moving the plotted observed recession parallel to the time axis until the observed recession matched one of the five selected percentile values. Also plotted on this figure are the maximum recession constants for each condition (as set out in Section 2.2). Equivalent plots for other sites are in the Supplementary Material.
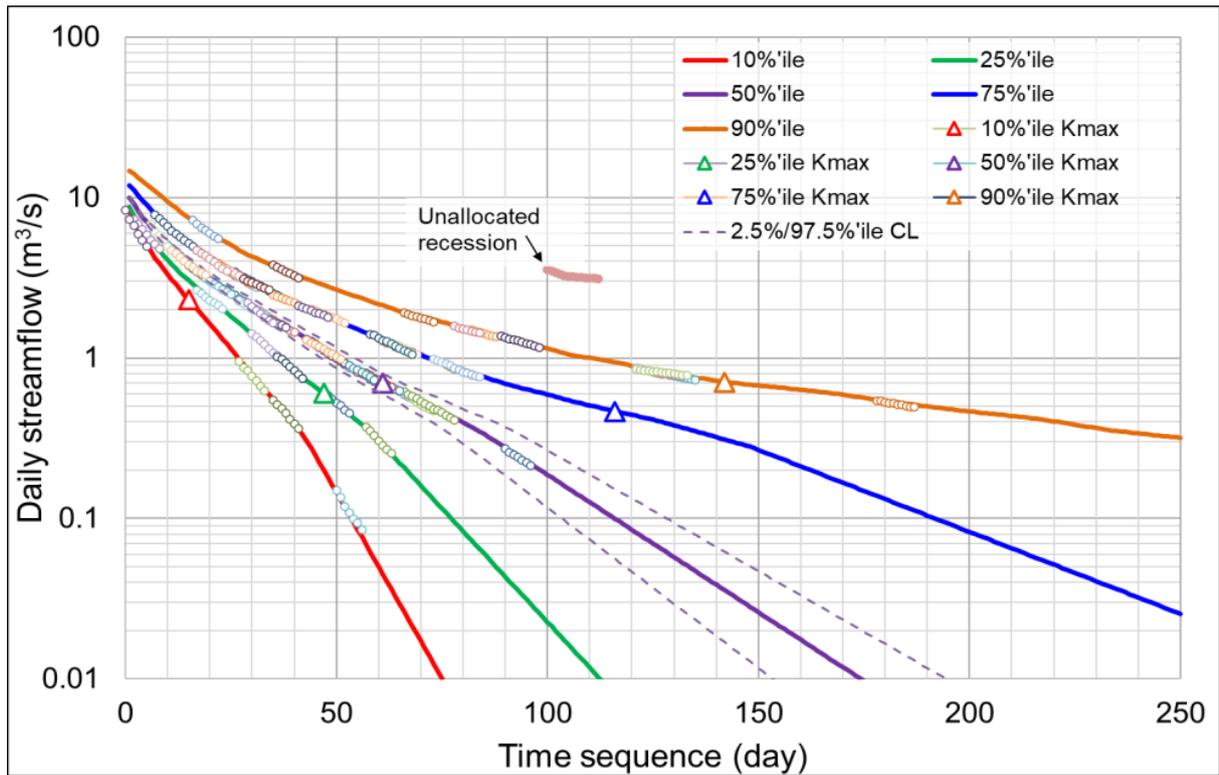
220

Figure 3 Comparison of daily MRCs computed using a constant bin correlation method with observed recessions during rainless periods for Gibbo River at Gibbo Park (401217). Three rainless days were required before data were acceptable in the analysis. The modelled recessions are for five percentile values: 10%, 25%, 50%, 75% and 90%. Maximum recession constants are located in the figure. The 2.5% and 95.5% confidence limits (CL) for the 50% MRC estimated using bootstrapping are also included. One

225 **acceptable recession was not allocated to one of the five MRCs.**

The number of plausible observed recessions plotted in the figures is listed in the last two columns of Table 1. The numbers varied from 24 for Northern Arthur to 65 for Gibbo whereas the final numbers plotted and allocated to a specific percentile MRC curve varied from 22 for Northern Arthur to 64 for Gibbo.

230

To assess the robustness of manual allocation of the observed daily recessions, for each recession in the Northern Arthur data (Figure S3, Supplementary Material) the magnitudes of the observed daily recession discharges were compared to the modelled recession discharges. Two metrics were computed based on the observed and modelled recessions: the standard correlation coefficient and the Nash-Sutcliffe Efficiency (Nash and Sutcliffe, 1970). The median correlation coefficient was

235 0.995 and the median Nash-Sutcliffe efficiency was 0.962, where the differences between the minimum and maximum of

11

these statistics were 0.015 and 0.315, respectively. Overall, the values for both metrics are high, confirming the adequacy of the manual allocation. However, it was observed that the lowest Nash-Sutcliffe value (NSE = 0.667) and another slightly higher value could be increased by shifting the observed recessions by one time step.

240 Figure 4 considers the influence of wet and dry periods on the plotted data for Gibbo River. The plots were compiled for the wet and the dry 6-months periods. The two periods were based on the mean monthly streamflows for Gibbo River at Gibbo Park in which the average streamflow during the wet period from July to December was 3.9 times the average streamflow during the dry period, January to June.
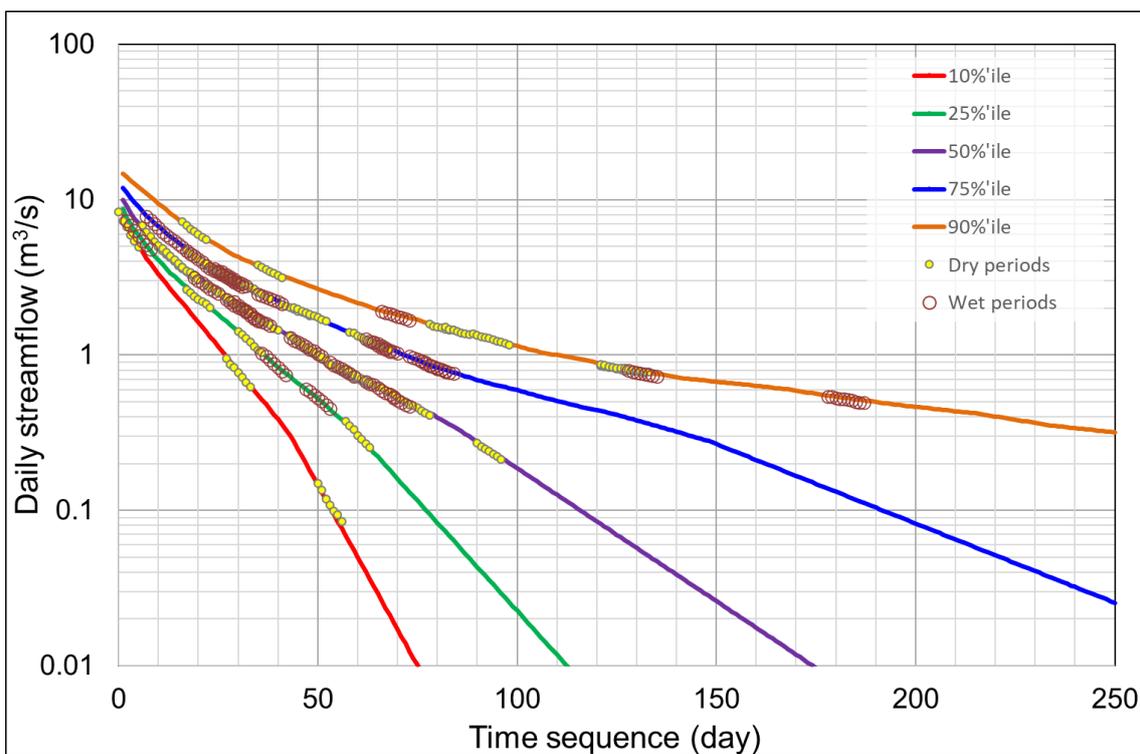

245

Figure 4 Comparison of observed daily recessions for data drawn separately from the wet 6-months and dry 6-months periods superimposed on the estimated MRCs for Gibbo River at Gibbo Park (401217).

12

4 Discussion

250 **4.1 Representation of natural variability**

The observed recessions for all four streams (shown in Figures 3 and 4, and in Supplementary Material, a total of 169 across the four streams) plot neatly on the computed MRCs. This is expected, of course, as both sets of results are drawn from the same data. Furthermore, the range of behaviour between the 10%'ile to 90%'ile MRCs provides much scope to ensure the observed recessions fit reasonably well to one of the five curves. The plots for Myall River (Figure S2) are an exception where

255 eight recessions were not allocated to one of the five MRCs. Most would have plotted on intermediate MRCs.

Two plots are provided for Northern Arthur. Figure 5(a) shows the recession data for the winter to mid-spring period whereas Figure 5(b) is for the summer to early autumn period. These two plots are discussed in detail later. The recession variability between summer and winter, which is characteristic of catchments in south-west Western Australia with perched water tables,

260 is discussed in detail by George and Conacher (1993). Noting that at the Lake Toolibin stream gauging station for Northern Arthur River, there are, on average, only 43 days of flow per year and so the number of plausible recessions is limited. It is also noted that the minimum flow plotted in these figures is about five times larger than the minimum that can be measured under field conditions (McMahon and Peel, 2019). It is comforting to note that for this stream the observed recessions in Figure 5(b) are, overall, consistent with the computed MRCs. The episodic nature of the Northern Arthur River hydrology is

265 evident in Figure 5 where the two of the three unallocated recessions are for climate conditions more extreme than the 10% to 90%'ile plotted range.
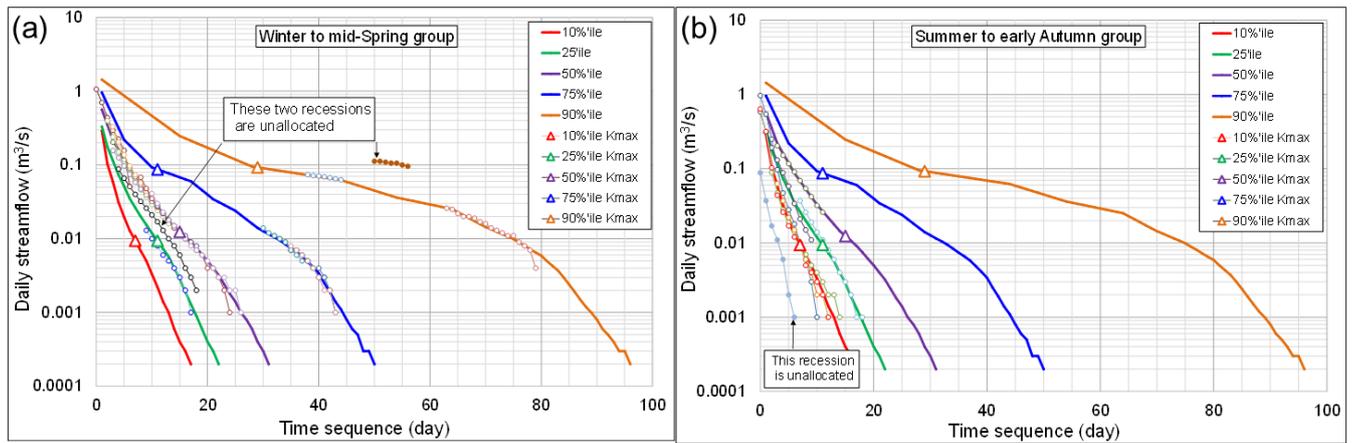
Figure 5 Comparison of seasonal daily MRCs for Northern Arthur River at Lake Toolibin Inflow (609010) with observed recessions during rainless periods for (a) winter to mid-spring and (b) summer to early autumn seasons. Three rainless days were required before data were acceptable in the analysis. The modelled recessions are for five percentile values: 10%, 25%, 50%, 75% and 90%. Maximum recession constants are shown in the figure. Two acceptable recessions were not allocated to one of the five MRCs.

We have not found plots similar to Figures 3 to 5 in the literature comparing observed recessions with probabilistic curves, although Kienzle (2006) identified two very different MRCs for a 7,675 km^2 watershed in Alberta, Canada. Fiorotto and Caroni (2013, Figure 6) incorporate a range of recessions as a function of probability by interpreting the master recession in terms of a stochastic process. On the other hand, Yang et al. (2019) developed separate MRCs for four flow regime conditions, high, moist, low, and dry and, separately, for the four climate seasons. The approach by Gao et al. (2023), inter alia, is similar to our method but they do not map the observed data to the developed recessions.

Our plots confirm that the adopted correlation method to estimating MRCs is a valid alternative to other approaches and is easily adapted to characterising natural variability and uncertainty. An important feature of Figures 3 to 5 is that the observed recessions extended beyond the day of their respective maximum recession constants, even for the extremely wet South Johnstone catchment with a mean annual runoff of more than 2000 mm/year (Figure S1) where there is evidence of transmission loss. Some studies (for example, Millares et al., 2009) involving recession analysis ($Q \sim t$) that produce $Q \sim t$ diagrams do not extend the time scale much beyond the maximum recession constant, presumably in the belief that the curve continues in a concave manner. We highlight this point as few journal papers dealing with $Q \sim t$ recession analysis address this important feature of an MRC.

14

Analysis of recessions separately for the wet and dry 6-month periods for Gibbo River (Figure 4) shows that the observed dry period recessions extend across the five computed MRCs whereas the observable recessions for the wet period cover mainly the 25, 50, 75 and 90%'ile MRCs. This distribution across the two periods is observed even though the dry 6-month period yields nearly one quarter the runoff generated during the wet period. The figure is important in that it demonstrates the difficulty in classifying catchment conditions in terms of general wet and dry periods, probably because we are examining the behaviour of individual events.

Another point to note relates to the confidence with which we can estimate the different percentile MRC curves. As pointed out earlier, we are suggesting the different percentile MRC curves represent the natural variability because of the initial storage in the aquifer and the configuration of the aquifers feeding the stream; in other words, the source of variability is the aleatory uncertainty due to antecedent conditions and its influence on a catchment with spatially heterogeneous physical properties.

However, our ability to identify the different percentile MRCs is limited by the period of available observations, where the uncertainty around the derived MRCs increases as the sample size decreases. This source of uncertainty represents the epistemic uncertainty due to sampling variability and can be characterised by non-parametric bootstrapping. To this end, the uncertainty around a given percentile MRC is characterised by resampling (with replacement) estimates of the recession constant within each bin. An example of the epistemic uncertainty around the median MRC for Gibbo River is shown by the (dashed) confidence lines in Figure 3. For the available data, it is seen that the epistemic uncertainty is much smaller than the aleatory uncertainty.

4.2 Hypothesis based on inductive reasoning

But what is the explanation for the variability exhibited in the Figures 3 to 5? Our proposed hypothesis is that, in the catchments we are considering, there are many sub-catchments (they have Strahler stream orders greater than three (Strahler, 1957)) with unconfined aquifers and delayed sub-surface flows. These sub-surface storages vary greatly in terms of dimensions, hydraulic properties, location and elevation relative to the nearest stream channel. This heterogeneity within a catchment combined with a varying climate is hypothesized to produce a continuum of MRCs as illustrated in the Figures 3 to 5.

Because Northern Arthur is, hydrologically speaking, a well-instrumented and researched catchment (Callow et al., 2007, 2020), it is used to assess a qualitative model explaining the observed variability (aleatory uncertainty) in the MRCs (Figure 5; see also Plates S1 and S2 in the Supplementary Material which show, respectively, the mid-western catchment and the

15

stream gauging station location). Two periods of activity are identified; the number of recessions over the winter to mid-spring period are twice that over summer to early autumn (Figure S6). Consider Figures 5(a) and 5(b) which show the recessions for Northern Arthur River. We deduce that the very steep 10%'ile MRC that occurs over about 15 days following rain on a very dry catchment occurs from an unconfined aquifer (denoted as A) with very high hydraulic conductivity. On the other hand, the considerably flatter 90%'ile MRC occurs after a very wet period and is likely fed from an aquifer (denoted as B) that exhibits a much more attenuated response to rainfall due to having either larger storage or lower hydraulic conductivity. For simplicity, we assume that these two aquifers, A and B, are in parallel and are the only groundwater sources discharging to the stream. After a very wet period that fills both aquifers, aquifer A will empty very quickly while aquifer B will dominate the recession. However, if aquifer A, the less attenuated aquifer, is located in the catchment such that after a long dry period there is sufficient rain to replenish it yet insufficient for aquifer B to discharge, a steep recession will result. This explanation must be tempered by noting that stream evaporation transmission losses probably will be high during the summer to early autumn periods (average area potential evapotranspiration (AAPE) ~5 mm/day) but much less during the winter to mid-spring periods (AAPE ~2.5 mm/day) (Wang et al., 2001). Adopting two parallel storages for aquifer modelling is not an unusual (see for example, Moore (1997) and Gao et al. (2017), although they assumed linear systems).

The above simple qualitative two-stage model of the surface water-groundwater connectivity proposed for the Northern Arthur catchment is not inconsistent with the three-stage surface water-groundwater connectivity and vertical recharge processes described by Callow et al. (2020). Their description is based on intensive instrumentation of the catchment and detailed analyses. As described by Callow et al. (2020), during the winter period soils saturate and macropores close, matrix flow dominates, and surficial aquifers become connected; although a vertical hydraulic gradient continues, the system acts as a semi-confined aquifer, and as the aquifers connect, a transition to the bottom-up groundwater discharge occurs. This description applies to the winter to mid-spring period resulting in the observed recessions depicted in Figure 5(a). From late spring, groundwater levels fall and, as the system dries, de-coupling between the surface and groundwater occurs, and macropores re-develop. Valley floor areas dry with large surface cracks. Top-down recharge occurs as a result of high infiltration facilitated by the macropores and surface flows. Observed recessions in Figure 5(b) are the result of these processes. In their discussion of the surface-subsurface processes involved, Callow et al. (2020) describe the transitions between the two main stages of low flow generation in Northern Arthur catchment. Referring to Figure 5, we surmise that some of the intermediate recessions (75%, 50% and 25%'iles) represent these transitions as the system passes from a wet period to a dry period and back again to the next wet phase.

16

5 Conclusion

This comparison between computed master recession curves (MRCs) and observed recessions for rainless periods confirms the usefulness of the computed MRC constructed using correlation between adjacent days. We hypothesise that the master recession curve is a continuum rather than a single average MRC and the variability across the continuum is the result of variable antecedent conditions in the unconfined aquifers and other sub-surface storages, their relative location, and the heterogeneity of their hydraulic properties. Our proposed approach is consistent with field data from the Northern Arthur catchment. The master recession curves examined herein support the notion that MRCs should be examined beyond the maximum recession constant to provide a more complete picture of the MRC than is portrayed in the published literature.

Acknowledgments

References

Ambroise B. Variable water-saturated areas and streamflow generation in the small Ringelbach catchment (Vosges Mountains, France): the master recession curve as an equilibrium curve for interactions between atmosphere, surface and ground waters. Hydrol. Process., 30, 3560–3577, 2016.

Arnold JG, Allen PM, Muttiah R, Bernhardt G. Automated base flow separation and recession analysis techniques. Groundwater, 33 (6), 1010–1018, 1995.

Barnes, BS. The structure of discharge-recession curves. Transactions AGU, 20, 721–725, 1939.

Bart R, Hope A. Inter-seasonal variability in baseflow recession rates: The role of aquifer antecedent storage in central California watersheds. J. Hydrol., 519,205-213, 2014.

Beran MA, Gustard A. A study into the low-flow characteristics of British Rivers, J. Hydrol., 35, 147-157, 1977.

Berhail S, Ouerdachi L, Boutaghane H. The use of the recession index as indicator for components of flow. Energy Procedia, 18, 741–750, 2012.

Boughton WC. Baseflow recessions. Austral. Civ. Eng. T., CE37, 9-13, 1995.

Boughton W. Master recession analysis of transmission loss in some Australian streams. Austral. J. Water Resour., 19 (1), 43–51, 2015.

Brodie RS, Hostetler S. A review of techniques for analysing baseflow from stream hydrographs. Proceeding of the NZHS305 IAHNZSSS, 2005 Conference, Auckland, New Zealand, 2005.

385 Brown HE. Characteristics of Recession Flows from Small Watersheds in a Semiarid Region of Arizona. Water Resour. Res., 1 (4), 517-522, 1965.

Brutsaert W, Nieber JL. Regionalized drought flow hydrographs from a mature glaciated plateau. Water Resour. Res., 13, 637–643, https://doi:7W0132, 1977.

Brutsaert W, Lopez JP. Basin-scale geohydrologic drought flow features of riparian aquifers in the southern Great Plains. 390 Water Resour. Res., 34 (2), 233-240, https://doi:0043-1397/98/97WR-030685, 1998.

Callow JN, Pope T, Coles NA. Surface water flow redistribution processes: Toolibin Lake natural diversity recovery catchment. CER 07/01 – SESE129, Report by the ARWA – Centre for Ecohydrology for the Department of Environment and Conservation, Perth, Western Australia, 2007.

Callow JN, Hipsey MR, Vogwill RIJ. Surface water as a cause of land degradation from dryland salinity. Hydrol. Earth Syst. 395 Sci., 24, 717–734, 2020.

Carlotto T, Chaffe PLB. Master recession curve parameterization tool (MRCPtool): Different approaches to recession curve analysis. Comput. Geosci.-UK, 132, 1–8, 2019.

Chapman TG. Modelling stream recession flows. Environ. Modell. Softw., 18, 683–692, 2003.

Chen X, Zhang Y-f, Xue X, Zhang Z, Wei L. Estimation of baseflow recession constants and effective hydraulic parameters 400 in the karst basins of southwest China. Hydrol. Res., 43 (1-2), 102-112 doi: 10.2166/nh.2011.136, 2012.

Chow VT, Maidment DR, Mays LW. Applied Hydrology. McGraw-Hill Book Co, 1988.

Duncan H. Baseflow separation - A practical approach. J. Hydrol., 575, 308–313, 2019.

Federer CA. Forest transpiration greatly speeds streamflow recession. Water Resour. Res., 9 (6), 1599-1604, 1973.

Fiorotto V, Caroni E. A new approach to master recession curve analysis. Hydrolog. Sci. J., 58 (5), 966-975, doi: 405 10.1080/02626667.2013.788248, 2013.

French R. Discussion on "Master recession analysis of transmission loss in some Australian streams" by W Boughton. Austral. J. Water Resour., 19 (2), 150-152, 2015.

Gao M, Chen X, Liu J, Zhang Z, Cheng Q. Using Two Parallel Linear Reservoirs to Express Multiple Relations of Power-Law Recession Curve. J. Hydrol. Eng., 22 (7), 04017013, 2017.

410   Gao M, Chen X, Singh SK, Dong J, Wei L. A probabilistic framework for robust master recession curve parameterization. J. Hydrol., 625, doi.org/10.1016/j.jhydrol.2023.12992, 2023.

George RJ, Conacher AJ. Mechanisms responsible for streamflow generation on a small, salt-affected and deeply weathered hillslope. Earth Surface Process & Landforms, 18, 291-309, 1993.

Gregor M, Malik P. Construction of master recession curve using genetic algorithms. J. Hydrol. Hydromech., 60 (1), 3–15 415   doi: 10.2478/v10098-012-0001-8, 2012.

Griffiths GA, McKerchar AT. Recession of streamflow supplied from channel bed and bank storage. J. Hydrol., (NZ) 49 (2), 99-109, 2010.

Griffiths GA, McKerchar AT. Comparison of a deterministic and a statistical model for predicting streamflow recession curves. J. Hydrol. (NZ), 54 (1), 53-62, 2015.

420   Grundy F. The ground-water depletion curve, its construction and uses. Assemblee Gen. De Bruxelles, International Association of Hydrological Sciences, 2, 213–217, 1951.

Hall FR. Base flow recession - a review. Water Resour. Res., 4 (5), 973-983, 1968.

Hameed M, Nayak MA, Ahanger MA. Event-based recession analysis for estimation of basin-wide characteristic drainage timescale and groundwater storage trends. Water Resour. Res., 59, e2023WR035829. https://doi.org/10.1029/ 425   2023WR035829, 2023.

Horner WW, Flynt FL. Relation between rainfall and runoff from small urban areas. Transactions ASCE, Paper 1926, 141–183, 1936.

Horton RE. The role of infiltration in the hydrologic cycle. Trans. Amer. Geophys. Union, 14, 446-460, 1933.

Institute of Hydrology. Low Flow Studies Report. Wallingford, UK., 1980.

430   James LD, Thompson WO. Least Squares Estimation of Constants in a Linear Recession Model. Water Resour. Res., 6 (4), 1062-1069, 1970.

Johnson EA, Dils RE. Outline for compiling precipitation, runoff, and groundwater data from small watersheds. Southeastern Forest Expt., Paper 68, 1956.

Kavousi A, Raeisi E. Estimation of groundwater mean residence time in unconfined Karst aquifers using recession curves. J. Cave Karst Stud., 77 (2), 108-119, 2015.

Kienzle S. The use of the recession index as an indicator for streamflow recovery after a multi-Year drought. Water Resour. Manag., doi: 10.1007/s11269-006-9019-1, 2006.

Kim M, Bauser HH, Bevan K, Troch PA. Time-variability of flow recession dynamics: Application of machine learning and learning from the machine. Water Resour. Res., 59, e2022WR032690. doi.org/10.1029/2022WR03269, 2023.

Lamb R, Beven K. Using interactive recession curve analysis to specify a general catchment storage model. Hydrol. Earth Syst. Sci., 1, 101-113, 1997.

Langbein WB. Some channel storage studies and their application to the determination of infiltration. Trans. AGU (EOS), 19, 435-447, 1938.

Latuamury B, Mardiatmoko, Kastanya A. Comparing master recession curves usings baseflow recession models. Indonesian J. Geog., 56 (2), 219-228, 2024.

Linsley RK, Kohler MA, Paulhus JLH. Hydrology for Engineers. New York-Toronto-London: McGraw-Hill Book Company Inc, 1958.

Linsley RK, Kohler MA, Paulhus JLH. Hydrology for Engineers. New York-Toronto-London: McGraw-Hill Book Company Inc Second edition, 1982.

Margreth M, Lustenberger F, Peter DH, Schlunegger F, Zappa M. Applying recession models for low-flow prediction: a comparison of regression and matching strip approaches. Natural hazards and Earth System Sciences, 2024-78, doi.org/10.5194/nhess-2024-78, 2024.

McMahon TA, Peel MC. Uncertainty in stage–discharge rating curves: application to Australian Hydrologic Reference Stations data. Hydrol. Sci. J., 64 (3), 255-275. doi:10.1080/02626667.2019.1577555, 2019.

McMahon TA, Nathan RJ. Baseflow and transmission loss: A review. WIREs Water, e1527, doi.org/10.1002/wat2.1527, 2021.

McMahon TA, Nathan RJ. Estimating hydraulic properties and residence times of unconfined aquifers. J. Hydrol., 654, 132861, 2025.

20

Millares A, Polo MJ, Losada MA. The hydrological response of baseflow in fractured mountain areas. Hydrol. Earth Syst. Sci., 13, 1261–1271, 2009.

460   Mizumura K. Analyses of Flow Mechanism Based on Master Recession Curves. J. Hydrol. Eng., 10 (6), 468-476, 2005.

Moore RD. Storage-outflow modelling of streamflow recessions, with application to a shallow-soil forested catchment. J. Hydrol., 198, 260–270, 1997.

Nash JE, Sutcliffe JV. River flow forecasting through conceptual models. Part I—a discussion of principles. J. Hydrol., 10 (3), 282–290, 1970.

465   Nathan RJ, McMahon TA. Evaluation of automated techniques for base flow and recession analysis. Water Resour. Res., 26 360 (7), 1465-1473, 1990.

Nimmo JR, Perkins KS. Episodic master recession evaluation of groundwater and streamflow hydrographs for water-resource estimation. Vadose Zone J., 17, 180050, doi:10.2136/vzj2018.03.0050, 2018.

O'Brien RJ, Misstear BD, Gill LW, Johnston PM, Flynn R. Quantifying flows along hydrological pathways by applying a new
470   filtering algorithm in conjunction with master recession curve analysis. Hydrol. Process., 28, 6211-6221, 2014.

Parra V, Munoz E, Arumí JL, Medina Y. Analysis of the behavior of groundwater storage systems at different time scales in basins of South Central Chile: A study based on flow recession records. Water, 15, 2503. https://doi.org/ 10.3390/w1514250, 2023.

Peel MC, Finlayson BL, McMahon TA. Updated world map of the Köppen-Geiger climate classification. Hydrol. Earth Syst.
475   Sci., 11, 1633–1644, 2007.

Pereira LS, Keller HM. Recession characterization of small mountain basins, derivation of master recession curves and optimization of recession parameters. Proc. Exeter Symposium, IAHS Publ., 138, 243-255, 1982.

Petras I. An approach to the mathematical expression of recession curves. Water SA, 12 (3), 145-150, 1986.

Posavec K, Parlov J, Nakić Z. Fully automated objective-based method for master recession curve separation. Ground Water,
480   48 (4), 598–603, 2010.

Rupp DE, Schmidt J, Woods RA, Bidwell VJ. Analytical assessment and parameter estimation of a low-dimensional groundwater model. J. Hydrol., 377, 143–154. https://doi.org/10.1016/j.jhydrol.2009.08.018, 2009.

Shaw EM. Hydrology in Practice. Third Edition, Chapman & Hall, London, 1994.

Singh SK, Griffiths GA. Prediction of streamflow recession curves in gauged and ungauged basins. Water Resour. Res., 57, doi:10.1029/2021WR030618, 2021.

Smakhtin VU. Low flow hydrology: a review. J. Hydrol., 240, 147-186, 2001.

Snyder WM. A concept of runoff-phenomena. Trans. Amer. Geophys. Union (EOS), 20, 725-738, 1939.

Snyder WM. Some possibilities for multivariate analysis in hydrologic studies. J. Geophys. Res., 67 (2), 721-729, 1962.

Strahler AN. Quantitative analysis of water shed geomorphology. Trans. Amer. Geophys. Union, 38 (6), 913-920, 1957.

Sujono J, Shikasho S, Hiramatsu K. A comparison of techniques for hydrograph recession analysis. Hydrol. Process., 18, 403–413, 2004.

Tallaksen LM. A review of baseflow recession analysis. J. Hydrol., 165, 349–370, 1995.

Toebes C, Strang DD. On recession curves 1: Recession equations. J. Hydrol. N.Z., 3 (2), 2-15, 1964.

Trotter L, Saft M, Peel MC, Fowler KJA. Recession constants are non-stationary: Impacts of multi-annual drought on catchment recession behaviour and storage dynamics. J. Hydrol., 630, 14pp. doi.org/10.1016/j.jhydrol.2024.130707, 2024.

Van Dijk AIJM. Climate and terrain factors explaining streamflow response and recession in Australian catchments. Hydrol. Earth Syst. Sci., 14, 159–169 https:// www.hydrol-earth-syst-sci.net/14/159/2010, 2010.

Wang QJ, Chiew FHS, McConachy FLN, James R, de Hoedt GC, Wright WJ. Climatic Atlas of Australia Evapotranspiration. Cooperative Research Centre for Catchment Hydrology and Bureau of Meteorology (Australia), 2001.

Whitaker AC, Chapasa SN, Sagras C, Theogene U, Veremu R, Sugiyama H. Estimation of base flow recession constant and regression of low flow indices in eastern Japan. Hydrol. Sci. J., 67 (2), 191-204, doi:10.1080/02626667.2021.2003368, 2022.

Yang D, Lee S, Lee G, Lim J, Lim KJ, Kim K-S. Estimation of Baseflow based on Master Recession Curves (MRCs) Considering Seasonality and Flow Condition. J Wetland Res., 21 (1), 34-42, 2019.

Yeh H-F, Huang C-C. Evaluation of basin storage–discharge sensitivity in Taiwan using low-flow recession analysis. Hydrol. Proc., 33, 1434-1447, 2019.

Code availability. The analyses described in this paper can be undertaken using standard spreadsheet software and does not require the development of bespoke code.

515